ELSEVIER

Journal of Molecular Catalysis A: Chemical 170 (2001) 175–186

JOURNAL OF MOLECULAR CATALYSIS A: CHEMICAL

www.elsevier.com/locate/molcata

Vibrational frequencies of CO adsorbed on silica supported Mo atoms from density functional calculations

Nuria López [a], Francesc Illas [a,*], Gianfranco Pacchioni [b]

[a] *Department Química Física i Centre Especial de Recerca en Química Teòrica, Martí i Franquès 1, E-08028 Barcelona, Spain*
[b] *Dipartimento di Scienza dei Materiali, Istituto Nazionale per la Fisica della Materia, Università di Milano-Bicocca, Via Cozzi 53, I-20125 Milano, Italy*

Received 13 September 2000; accepted 18 January 2001

Abstract

The interaction of CO with silica supported molybdenum atoms has been studied by means of density functional calculations and cluster models. Experimentally two bands in the IR spectra of adsorbed CO have been observed at 2170 and 1990 cm^{-1} with vibrational shifts of +27 and −153 cm^{-1}, respectively, with respect to the gas-phase molecule, the peak at +27 cm^{-1} has been related to the presence of neutral Mo atoms anchored to two oxygen atoms of the SiO_2 substrate. Possible reactive sites at the Mo/SiO_2 interface have been explored as candidates for CO adsorption. Mo atoms in various formal oxidation states, from +II to +VI, have been considered. Both molecular and cluster models of the Mo/SiO_2 interface have been employed. The analysis shows that a neutral Mo(II) atom, proposed to be responsible for the blue-shift of ν(CO), is not likely to be the origin of the IR band at 2170 cm^{-1}. Only Mo atoms in high oxidation states or Mo cations carrying a real positive charge can account for the positive shifts in the CO frequency.

Keywords: Calculations (ab initio); Vibrational frequency; Silica; Carbon monoxide; Molibdenum

1. Introduction

Supported metals form a broad class of technologically important catalysts [1]. These catalysts are usually synthesized by reaction of a metallic salt with the hydroxylated surface of an oxide, typically silica or alumina. However, the largest amount of theoretical studies in this area is dealing with metals deposited on non-defective and hydroxyl-free highly ionic surfaces, e.g. MgO [2].

Molybdenum-based catalysts are involved in several reactions that include partial oxidation and strong reductions [3]. This chemical ability of Mo is due to the large number of available oxidation states (OS). The concentration of Mo atoms in a given OS in the catalyst depends heavily on the working conditions. For instance, activation procedures usually result in a complex distribution of species in several valence states [4]. Recently, different procedures to synthesize Mo-based catalyst with a narrow OS distribution have been described [5,6]. In these schemes, it is possible to tune the selected oxidation state necessary for a given reaction. One of these methods is described in Scheme 1. Yermakov and Iwasawa reported synthetic routes that allow the creation of uniform surface sites that can evolve to Mo(IV) and Mo(VI) in a discrete way [5,6] (here we adopt the notation Mo(II) to indicate the formal +II oxidation state of a

* Corresponding author. Tel.: +34-93-402-1229; fax: +34-93-402-1231.
E-mail address: f.illas@qf.ub.es (F. Illas).

1381-1169/01/$ – see front matter
PII: S1381-1169(01)00058-9

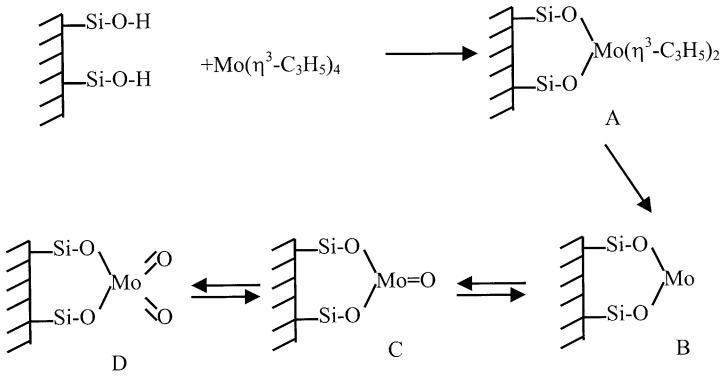

Scheme 1.

neutral system, and Mo^{2+} to indicate a real cation). More specifically, the reaction of $Mo(\eta^3\text{-}C_3H_4)_4$ with hydroxyl groups at the amorphous silica surface is supposed to lead to a structure with an isolated Mo atom linked by two ≡Si–O– groups to the silica network, see structure A in Scheme 1. The subsequent hydrogenation may lead to the formation of structure B, another kind of Mo(II); oxidation in mild conditions may lead to Mo(IV)-like structures, while in stronger oxidation conditions Mo(VI) forms. These last steps are reversible upon H_2 exposure.

From XPS measurements, it has been found that a mixture of different oxidation states coexist in compound C and, to a smaller extent, in B [7]. The stretching frequencies of CO adsorbed on samples containing species B, C and D, have been determined by FT-IR [8]. CO vibrational frequencies are known to be strongly dependent on the electron density of the metal and very sensitive to details of the electronic structure of the substrate, a particularly important role is that of the metal d orbitals and of the associated back-donation mechanism. Following results in [8], the adsorption of CO on species B results in a final frequency for CO of 2170 cm^{-1}, blue-shifted by 27 cm^{-1} with respect to the free gas-phase CO molecule, 2143 cm^{-1}. In addition, it has been suggested that H_2 can block the adsorption sites for CO and that products C and D do not show peaks corresponding to CO bands. If the sample B is in contact with CO for a longer period, a new band at 1420 cm^{-1} evolves slowly, the intensity of this peak is almost constant after 2 h, does not depend on the amount of Mo, and is located in the region corresponding to carbonate groups [9]. When considering longer times, 24 h, a peak at 1990 cm^{-1} appears and increases in intensity with time in contact with CO while the corresponding peak at 2170 cm^{-1} decreases sharply. If light is present, other bands appear at 2120, 2090, 2030 cm^{-1}, while if the sample is kept in dark, the interchange between bands at 2170 and 1990 cm^{-1} is strongly reduced. The band at 2170 cm^{-1} has been assigned to isolated Mo(II) in the catalyst by Brito and Griffe [8]. Zaki et al. and Louis et al., however, have assigned these peaks to the presence of Mo(III) [10,11]. At low temperatures two maxima at 2155–2133 cm^{-1} for CO physisorbed on silica at 77 K [11] have been observed; the corresponding binding energy is about 0.1 eV [12–15] while calculations for the CO molecule with models of isolated hydroxyl groups on silica lead to values for the harmonic shift of about +20 cm^{-1} [16]. Finally, the adsorption of $Mo(CO)_6$ on SiO_2 leads to two bands at 1990 and 2020 cm^{-1} [11].

Aim of this work is to analyze the assigned frequencies by comparing the available experimental data for the adsorption of CO on Mo/SiO_2 with results from density functional theory (DFT) quantum chemical models of this complex system. It is now well established that modern quantum-chemical methods are able to reproduce with satisfactory accuracy the vibrational energies and in particular the vibrational shifts of molecules adsorbed on transition metals. We have determined the C–O adsorption geometry and vibrational frequency for a series of systems where the OS

of Mo is increased from +II to +VI. The effect of having charged species on the surface has also been analyzed. We have considered first a series of molecular models where the Mo atom is bound to O or OH groups, in a second series of calculations, the support has been explicitly included by means of cluster models of the SiO_2 surface.

2. Computational approach

The computational approach adopted follows our previous works on supported metals [17–21]. This is based on the use of finite cluster models and of DFT in a localized basis set. The exchange-correlation functional employed is the B3LYP [22,23], since it has been shown that it represents in a proper way the interactions taking place at the interface between a metal atom and an oxide surface [24,25]. In some cases, the electronic structure of the resulting models has a marked open-shell character. When this is the case, the unrestricted, UB3LYP, formalism has been used to obtain the self-consistent Kohn–Sham density. The final electronic states, thus, obtained do not have a definite spin multiplicity. Nevertheless, the usual notation — singlet, doublet, triplet, etc. — will be used to denote the electronic states corresponding to a given number of unpaired electrons.

In order to analyze the effect of electronic contributions to the vibrational frequency of adsorbed CO, a series of small Mo-containing molecular models has been considered. In a second step, more realistic models of the silica surface have been derived from the structure of α-quartz. The choice to use the α-quartz crystalline phase of silica instead of the amorphous one may look somehow arbitrary, since the structure of the support in a real catalyst is not known in detail and depends on the history of the sample, e.g. preparation procedure. For instance, distances between hydroxyl groups at the silica surface show a continuous range of values depending on the preparation temperature [26]. However, since the formation of a bond between the OH groups and the incoming Mo organometallic complex is a local phenomenon, it can be studied with cluster models derived from the quartz structure.

The model that describes the hydroxylated surface of the SiO_2 network contains two SiO_4 tetrahedra. It simulates two adjacent or vicinal silanol groups on two neighboring silicon atoms, the model is referred to as 2(T-OH). The selection of such small cluster model is justified both from the analysis of experimental data [27] and from theoretical studies [17,18]. The two-tetrahedra SiO_4 cluster is the minimum structure that can provide the correct coordinative pattern for the deposited metal. The unpaired bonds originated by the cut of the two tetrahedra structure from the solid have been saturated with hydrogen atoms [28]. The final stoichiometry is $(H_tO)_2Si–(OH)–O–Si(OH_t)_2(OH)$, where H_t indicates a terminal saturating H atom. In the geometry optimizations, the terminal H atoms have been fixed so as to reproduce the effect of the mechanical restrictions induced by the solid matrix in a simple, but rather effective, way. The positions of all the other atoms of the cluster, Si, O, Mo and C have been fully optimized by means of analytical gradients of the total energy.

The Kohn–Sham orbitals have been expanded by means of localized contracted Gaussian type orbitals. The basis set for the O and Si atoms have been described by a 6-31G(d) basis set [29] while H terminal atoms on the silica model employ a smaller 3-21G basis set [30], for the Mo atom the representation includes a relativistic pseudopotential and the basis set described by Hay and Wadt in a double-zeta representation [31]. For CO, we used the 6-311G(d) basis set [32]. For the molecular models, the determination of the vibrational frequencies has been performed within the harmonic approximation by computing the second derivatives of the total energy at the fully optimized geometry. For supported metals, the mass of the H_t atoms in the SiO_2 models has been set to a very large value so as to uncouple the vibrations of the model from the rest of the solid. The calculations have been performed with the Gaussian 94 program [33].

3. Results

3.1. Mo molecular models

The relation between the Mo OS and the frequency of an adsorbed CO molecule has been subject of several analyses. For instance, Zaki et al. [10] noticed that it is possible to reproduce the vibrational shifts of an adsorbed CO molecule on molybdena supported on various oxides assuming that the shift is related

Table 1
Electronic properties of CO adsorbed on molecular models of Mo atoms in various oxidation states[a]

Species	Model	Symmetry	E_r (eV)	D_e (eV)	$\Delta\nu$ (cm^{-1})
Mo(II)	$Mo(OH)_2$	$^1A_1$	0.85	2.35	−294
Mo(II)	$Mo(OH)_2$	$^3B_2$	0.00	1.51	−224
Mo(III)	$Mo(OH)_3$	^2A	0.00	1.59	−211
Mo(IV)	MoO_2	$^1A'$	0.60	1.57	−112
Mo(IV)	MoO_2	$^3A''$	0.00	1.22	−61
Mo(V)	$MoO_2(OH)$	$^2A'$	0.00	0.57	−81
Mo(VI)	MoO_3	$^1A'$	0.00	1.14	+76
Mo(VI)	MoO_3	$^3A''$	1.54	0.72	−77
$Mo(III)^+$	$[Mo(OH)_2]^+$	$^2A_1$	0.00	1.83	−20
$Mo(V)^+$	$[MoO_2]^+$	$^2A''$	0.00	1.87	+79

[a] E_r: relative energy with respect to the ground state; D_e: CO adsorption energy; $\Delta\nu$: harmonic CO vibrational frequency shift with respect to the free molecule. Computed values for free CO: $r_e = 1.127$ Å, $\nu = 2221\ cm^{-1}$.

to the electric field associated to the presence of a Mo^{n+} ion. Unfortunately, as we will show below, while this approach works quite nicely for CO adsorbed on non-transition metal cations [34], it is not adequate in the case of metal atoms with a filled or partially filled d shell because of the occurrence of a substantial back donation. In order to investigate these effects, we have studied the adsorption of CO on molecular models representing different OSs of Mo, these have been generated by adding O atoms or OH groups to a single Mo atom, the formal OS has been deduced following the usual rules to assign a −II value to O and a −I value to OH. OH groups are the closest analogues to the real situation where Mo is bound to O–Si groups. However, to achieve some of the OSs without increasing the coordination number of Mo, we have used only O atoms for larger oxidation states.

The smallest molecular model that would simulate system B, tentatively assigned to Mo(II) (Scheme 1), is $Mo(OH)_2$. The relative energetic position of two spin states is reported in Table 1, with the triplet being 0.85 eV lower than the singlet. The $Mo(OH)_2$ structure, together with some geometric parameters, for both singlet and triplet states is shown in Fig. 1. The interaction energy with a CO molecule is rather strong, 1.51 eV for the triplet state and 2.35 eV for the singlet one. These energy differences have been calculated with respect to their corresponding spin state. Since, as stated above, the triplet stable is more stable than the singlet by 0.85 eV but the binding energy in the singlet is 0.84 eV higher, in $CO/Mo(OH)_2$, the singlet and the triplet states are nearly degenerate. The CO equilibrium bond distance provides a direct measure of the extent of metal to CO back-bonding. For the singlet case, it is about 1.17 Å, while for the triplet it is 1.16 Å. In both cases, it is longer than in the free molecule where at the same level of theory one finds 1.127 Å. This is already indicative of a considerable back-donation. The Mo–CO distance is shorter for the singlet configuration than for the triplet, 1.87 versus 1.94 Å, consistent with the stronger binding. The harmonic CO stretching frequency is significantly red-shifted, by 294 cm^{-1} in the singlet state and by 224 cm^{-1} in the triplet, respectively, with respect

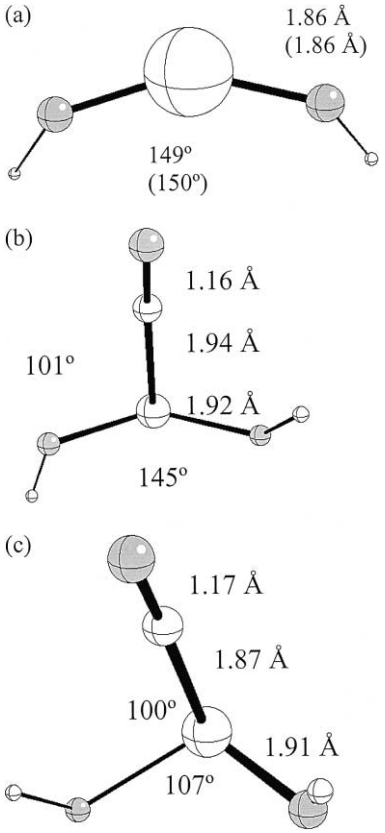

Fig. 1. Structure of (a) the $Mo(OH)_2$ molecular model, (b) the product of CO adsorption (singlet state), and (c) the product of CO adsorption (triplet state). Distances in Å, angles in degrees. Values in parenthesis are for the triplet state.

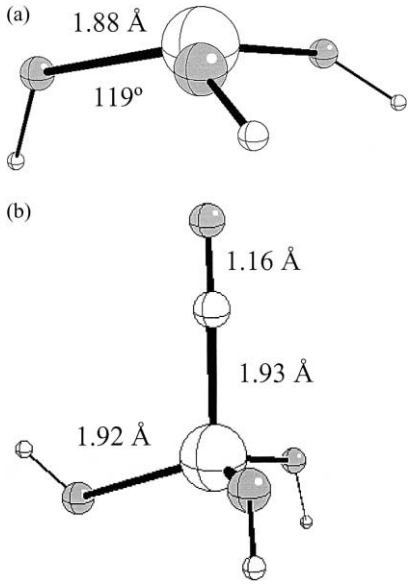

Fig. 2. Structure of (a) the $Mo(OH)_3$ molecular model, and (b) the product of CO adsorption. Distances in Å, angles in degrees.

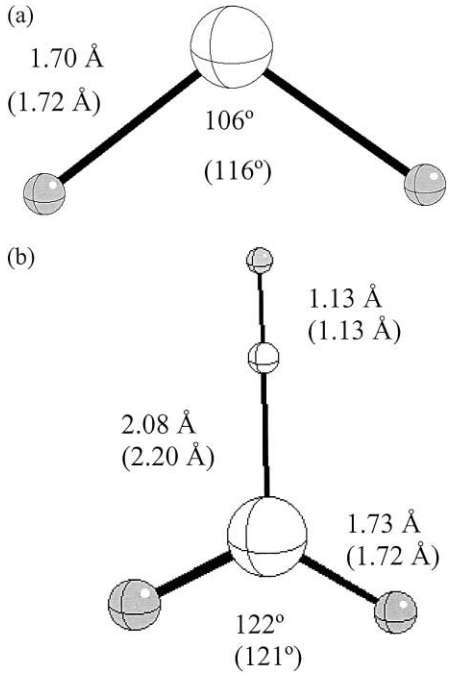

Fig. 3. Structure of (a) the MoO_2 molecular model, and (b) the product of CO adsorption. Distances in Å, angles in degrees. Values in parenthesis are for the triplet state.

to the calculated reference for the free CO molecule, 2221 cm^{-1}. Notice that for the gas phase molecule, the experimental harmonic frequency is 2170 cm^{-1} while 2143 cm^{-1} is the anharmonic value [35]. Compared to the experimental band appearing at 2170 cm^{-1}, the computed shifts of -294 and -224 cm^{-1} not only have the wrong sign, but are almost one order of magnitude larger in absolute value than the experimental shift of $+27$ cm^{-1} assigned to Mo(II).

The introduction of a third (OH) group leads to the formation of $Mo(OH)_3$, the model for the Mo(III), which has a doublet ground state. The bare Mo complex and the product of adsorption with CO are shown in Fig. 2. CO is bound to $Mo(OH)_3$ by 1.57 eV with a Mo–CO distance of 1.93 Å, the CO frequency shift is -211 cm^{-1} (Table 1). All these values are very close to those obtained for the triplet state of $Mo(OH)_2$. Therefore, even a Mo atom in a +III OS maintains a strong back bonding ability shown by the red-shift of more than 200 cm^{-1}. A MoO_2 molecule is the model of a Mo(IV) neutral atom, and its structure is shown in Fig. 3. For this system both singlet and triplet states have been explored, the triplet being more stable by about 0.6 eV, see Table 1. The interaction energy with CO, however, is again larger by 0.35 eV for the singlet than for the triplet state, 1.57 versus 1.22 eV, thus, the complex with CO keeps an open shell ground state structure. The Mo–CO distance increases and becomes larger than 2 Å (Fig. 3). The CO stretching frequencies are still red-shifted by 112 and 61 cm^{-1} for the singlet and triplet states, respectively (Table 1). Thus, even a low-coordinated Mo(IV) atom exhibits a substantial back donation to CO, contrary to what one would expect from chemical intuition.

The Mo(V) oxidation state is represented by the $MoO_2(OH)$ molecule (Fig. 4). The resulting system shows an unpaired electron and has been computed in a doublet state. The products of CO adsorption are also represented in Fig. 4. The interaction energy with CO, 0.57 eV, is much smaller, almost one-half, than for the previous system. This can be due to the reduction of the metal d-population which implies a smaller contribution to the bonding from back-donation mechanisms. This correlates with the metal–carbon distance, 2.16 Å, much larger than in previous cases and with a shorter C–O distance, 1.12 Å. As a result, the vibra-

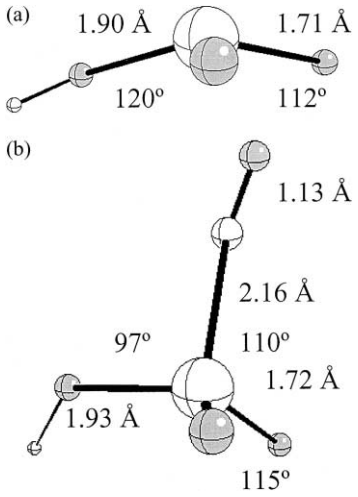

Fig. 4. Structure of (a) the $MoO_2(OH)$ molecular model, and (b) the product of CO adsorption. Distances in Å, angles in degrees.

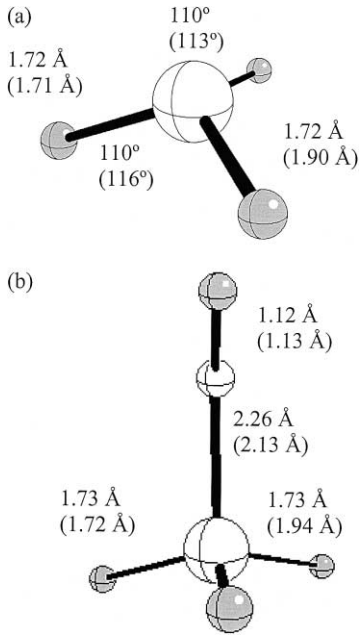

Fig. 5. Structure of (a) the MoO_3 molecular model, and (b) the product of CO adsorption. Distances in Å, angles in degrees. Values in parenthesis are for the triplet state.

tional frequency is only $80\,cm^{-1}$ smaller (red-shifted) than the one calculated for free CO. In this case, we are in the presence of a relatively weak bond, but still of a red-shift of the frequency. It is somewhat surprising that despite the long Mo–CO distance, the overlap of the metal d orbitals with the CO antibonding levels is sufficiently large to give rise to a significant red-shift in ν(CO).

A Mo(VI) center has been represented by a MoO_3 molecular model. This molecule has the same stoichiometry of some of the Mo particles that may exist in the real catalysts. As can be seen in Table 1, the singlet state is much more stable than the triplet one, by about 1.5 eV. The products of CO adsorption are shown in Fig. 5. The interaction energy is 1.14 eV for the singlet ground state, and 0.72 eV for the excited state triplet. The interaction is, therefore, weaker than on most of the other complexes considered so far with the exception of $MoO_2(OH)$ (Table 1). This is reflected also in the metal to adsorbate distances which becomes rather larger, >2.2 Å. For the singlet state, the C–O distance is small, 1.12 Å, and the vibrational frequency, $2297\,cm^{-1}$, is larger (blue-shift) that the gas-phase value by $76\,cm^{-1}$, for the triplet state the CO frequency is still red-shifted by $70\,cm^{-1}$. This in part connected with the fact that in the triplet state the Mo–CO distance is shorter than in the singlet (Fig. 5). Indeed, the distance in the triplet state, 2.13 Å, is close to that found on $MoO_2(OH)$, and also the $\Delta\nu$, $-77\,cm^{-1}$, is comparable. One can indirectly deduce that at a Mo–CO distance of more than 2.2 Å, the metal d_π-CO $2\pi^*$ overlap is virtually zero and the shift is dominated by electrostatic effects (see below), at distances shorter than 2.2 Å the d_π-CO $2\pi^*$ overlap starts to occur. This balance leads to a positive shift in the CO frequency which is peculiar for the Mo(VI) OS.

Some trends can be recognized from these results. To a higher OS of the metal, i.e. to a larger number of oxygen or hydroxyl groups, corresponds a longer Mo to CO distance, a shorter C–O distance, and a larger value of the CO frequency. The back-donation mechanism which is responsible for the strong red-shift of CO stretching mode when CO interacts with metal atoms, is significantly reduced by decreasing the electronic population in the d orbitals. Not surprisingly, a higher OS implies less electron density on the d orbitals and a reduced electron transfer to the $2\pi^*$ orbitals of CO. What is less intuitive is that even for a Mo atom in high OS, +IV or +V, the shift in the CO frequency is still large and negative. Only when CO is

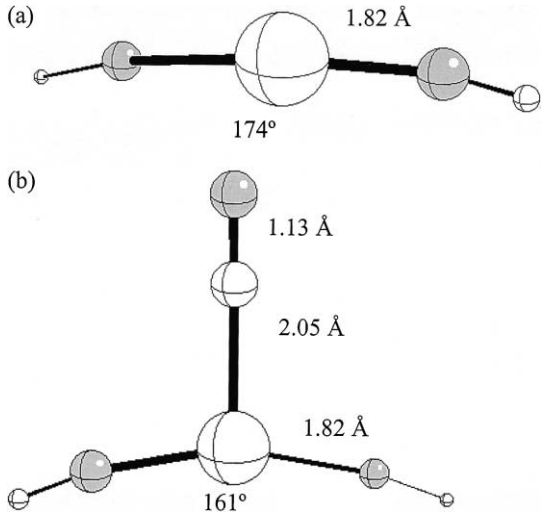

Fig. 6. Structure of (a) the $[Mo(OH)_2]^+$ molecular model, and (b) the product of CO adsorption. Distances in Å, angles in degrees.

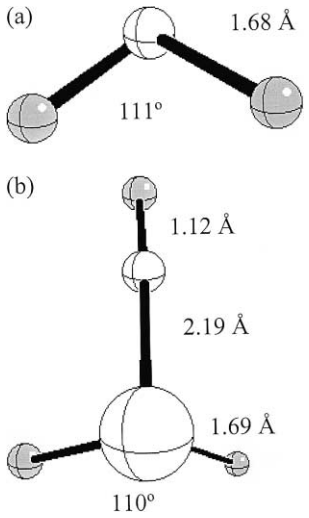

Fig. 7. Structure of (a) the $[MoO]^+$ molecular model, and (b) the product of CO adsorption. Distances in Å, angles in degrees.

bound to the MoO_3 molecule (singlet state), a positive shift is predicted from DF calculations. This is due to the particular electronic structure of the molecule and to the high formal OS of the metal. However, since species B in Scheme 1 is not a completely oxidized species and no contribution of Mo(VI) has been found in XPS, it seems that a simple change in the number and nature of the ligands around the Mo atom does not account for the observed blue-shift in the CO stretching frequencies for CO on Mo/SiO_2.

We have seen that only the most oxidized species show a shift in the vibrational frequency close to the observed value. In principle, one cannot rule out the possibility that charged structures form at the interface. Charged ions induce an electric field which interacts electrostatically with the CO dipole moment causing important displacements in the CO vibrational frequency [10,34]. In order to verify this point, two different systems have been considered to represent charged structures. The first one leads to a +III oxidation state of the Mo atom $[Mo(OH)_2]^+$, while the second corresponds to Mo(V) $[MoO_2]^+$ (see Figs. 6 and 7). For the first structure $[Mo(OH)_2]^+$, the computed interaction energy with CO is about 1.8 eV (Table 1). The charge induces an electric field which interacts with the CO molecule, but also causes a contraction of the d orbitals on Mo and a reduction of the Pauli repulsion. As a consequence, the CO distance becomes 1.13 Å and the vibrational frequency is very close to that of the free molecule, but still red-shifted by about $20\,cm^{-1}$. In the case of $[MoO_2]^+$, on the contrary, the shift of the CO frequency is large and positive, $+79\,cm^{-1}$ (Table 1). Note that in this latter complex, despite the large Mo–CO distance, 2.19 Å, the interaction is strong, 1.87 eV. This is due to the fact that the loss in metal–CO bonding due to the reduced back-donation is compensated by the electrostatic interaction with the local electric field.

From these data, two general conclusions can be drawn. Neutral Mo atoms, even in high OS give rise to red-shifts in the CO vibrational frequency. The only exception is that of Mo(VI) in MoO_3 where a positive shift is computed for the singlet ground state. For the lower OSs, the shifts are negative and large. Models of Mo(II), for instance, result in a reduction of the CO stretching frequency of up to $300\,cm^{-1}$, suggesting a strong back bonding ability of the transition metal atom. Positively charged complexes can induce positive shifts in the CO frequency provided that the OS of the metal is medium or high. These conclusions are based on very simple molecular models, with little resemblance to the real silica substrate. However, these oversimplified models have proven to be useful to provide guidelines for the construction of models that take

into account the presence of the support. These more realistic models of the support are considered in the next section.

3.2. Silica supported Mo

From XPS measurements of the position of the 3d band [7] and from stoichiometric measurements of H_2/O_2 consumption [8], it has been concluded that structure B corresponds to a large extent to a Mo in a +II oxidation state. However, a significant fraction, ≈10% of Mo(IV) contribution has been found even when performing two oxidation–reduction cycles [7]. Following stoichiometric measurements, structure C should correspond to an average OS (IV), but the broad 3d peak in the XPS spectrum has been fitted with contributions from different oxidation states from Mo(III) to Mo(VI). Thus, species C does not represent a unique OS. Further oxidation produces Mo(VI) as a single isolated species and has been proposed to be tetrahedrally coordinated.

We have considered four possible candidate structures for species B in Scheme 1 (see Figs. 8–11), and we have studied their reactivity towards CO, starting with the 2(T-OH) model, the final structure for the adsorbed Mo results in a three-member ring [$(HO)_4OSi_2O_2$–Mo] (Fig. 8) (here we adopt the usual notation for quartz where a *n*-member ring corresponds to *n*-Si–O units). These kinds of close ring structures are very stable and have already been found in the theoretical study of interaction of Cu, Pd and Cs metal atoms with non-bridging oxygens at the silica surface [18]. A non-bridging oxygen radical, ≡Si–O•, can be seen as the product of the homolytic scission of a surface silanol group, ≡Si–OH → ≡Si–O• + H•. The Mo atom in [$(HO)_4OSi_2O_2$–Mo] is bonded to two surface oxygens with distances of about 1.89 Å. Notice that these are rather short distances, similar to those found for single Mo–O bonds in the molecular models (Figs. 1–7). With this model of the SiO_2 surface, we do not see additional minima. The triplet state is more stable than the singlet one by 0.83 eV (Table 2). This is practically the same energy difference found between singlet and triplet in $Mo(OH)_2$, supporting the analogy of the molecular models with the surface models.

For the interaction energy of the CO molecule with [$(HO)_4OSi_2O_2$–Mo] (see Fig. 8), the adsorption

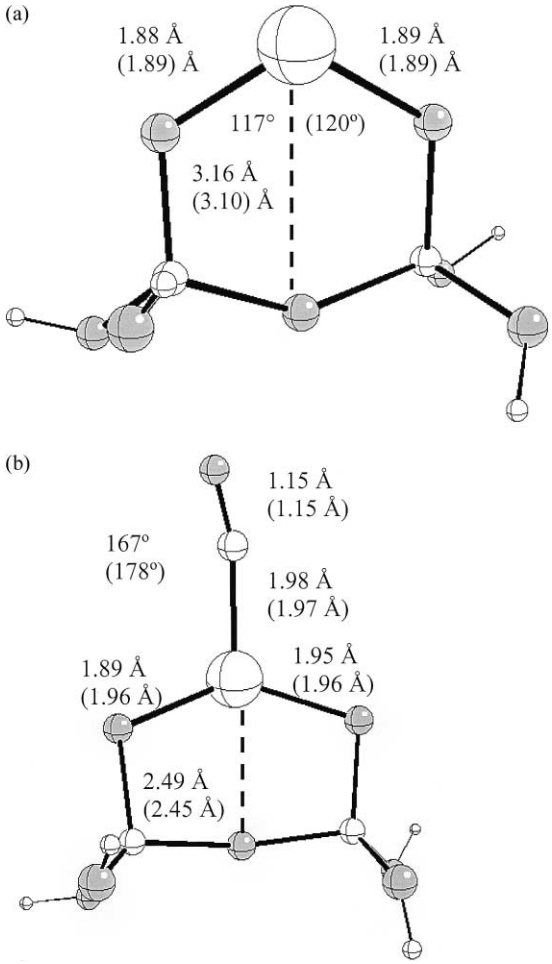

Fig. 8. (a) The [$(HO)_4OSi_2O_2$–Mo] cluster model, and (b) the product of CO adsorption. Distances in Å, angles in degrees. Values in parenthesis are for the triplet state.

energy is similar for the singlet and triplet states, 1.8–1.9 eV. The addition of the CO molecule results in a strong relaxation of the Si–O–Mo ring which is indicative of the nature of the Mo–CO bonding. In fact, while in the SiO_2–Mo complex, the distance between Mo and the non-bonded O atom of the ring is 3.1 Å (Fig. 8(a)), in the SiO_2–Mo–CO surface complex this distance decreases to 2.49 Å (Fig. 8(b)). This is due to the dative bonding formed between a lone pair on the bridging oxygen and the electron deficient Mo(II) atom. This bonding, which is not present in absence of CO, is a clear sign of the strong depletion of charge

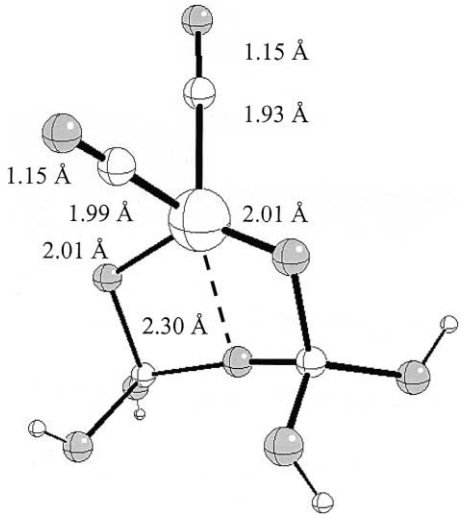

Fig. 9. The $[(HO)_4OSi_2O_2–Mo]$ cluster model of a supported Mo interacting with two CO molecules (singlet state). Distances in Å.

on Mo due to the back donation to the CO molecule. The reduced electron density and the increased positive charge on Mo favor the formation of the dative bonding O → Mo. As a consequence, an O atom of the ring becomes effectively three-coordinated (O_{3c}). The strong back bonding from Mo to CO is shown also by the calculated CO frequency, 1999 cm^{-1} for the singlet and 2006 cm^{-1} for the triplet state, with a red-shift of more than 200 cm^{-1}, typical for CO bound to metal atoms in low OS. Notice that also this result is similar to that obtained with a molecular $Mo(OH)_2$ model. Thus, it is not possible to support structure B as responsible for the frequency reported in [8], 2170 cm^{-1}. On the contrary, it is more likely that this structure generates the band observed after light treatment at 1990 cm^{-1}. Since the differences in frequencies are small for the singlet and triplet state, we have computed the interaction of the singlet state with a second CO molecule in order to form a geminal $Mo(CO)_2$ species (Fig. 9). The adsorption energy of the second CO molecule is still favorable, 1.86 eV. Removing the two CO molecules has an energy cost of 3.69 eV (cf. Table 2). Apparently, on Mo there is enough electron density to give rise to a considerable back donation towards both CO molecules. As a consequence, the dative bonding from the ring O atom is reinforced and the Mo–O_{3c} distance decreases to

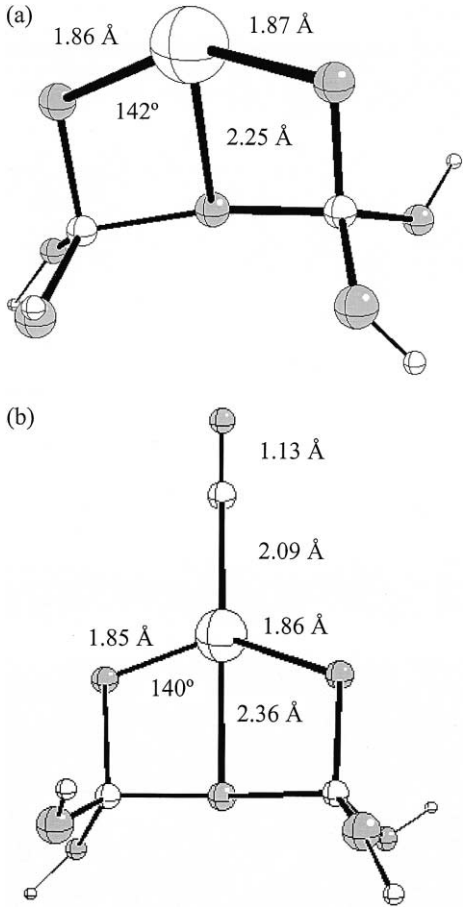

Fig. 10. (a) The $[(HO)_4OSi_2O_2–Mo]^+$ cluster model, and (b) the product of CO adsorption. Distances in Å, angles in degrees.

2.30 Å (Fig. 9). As expected for a geminal carbonyl, two frequencies are computed for the C–O stretching, both red-shifted by 224 and 155 cm^{-1} (Table 2). Thus, even a geminal dicarbonyl complex does not account for the observed band at 2170 cm^{-1}.

The charged $[(HO)_4OSi_2O_2–Mo]^+$ surface species and its complex with CO have also been studied (see Fig. 10). Here, even in absence of adsorbed CO, the presence of a positive charge results in a strong relaxation of the ring and in a rather short Mo–O_{3c} distance. Differently from the previous case, the addition of a CO molecule now results in the elongation of the Mo–O_{3c} bond (Fig. 10). This is probably due to the fact that in presence of a fourth ligand, the positive charge is distributed over more centers and the

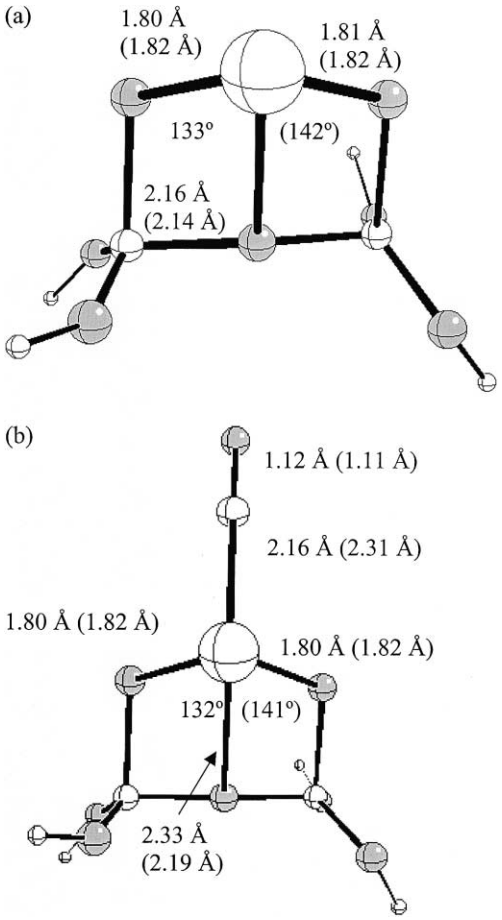

Fig. 11. (a) The $[(HO)_4OSi_2O_2–Mo]^{2+}$ cluster model, and (b) the product of CO adsorption. Distances in Å, angles in degrees. Values in parenthesis are for the triplet state.

electrostatic interaction with O_{3c} is reduced. The CO binding energy, 1.73 eV is large and comparable to that found in $[Mo(OH)_2]^+$ and the stretching frequency, 2180 cm^{-1}, with a $\Delta\nu = -41\,cm^{-1}$, is also similar to the molecular analogue (see Tables 1 and 2). The value of ν(CO) is mainly due to the electrostatic terms which arise when charged species are into play, but the shift is still opposite to what is observed for the band at 2170 cm^{-1}. One has to conclude that despite the positive charge, some back bonding is still occurring.

Divalent charged species such as $[(HO)_4OSi_2O_2–Mo]^{2+}$ may also exist, and about a 10% of Mo atoms in the real catalyst are indeed Mo(IV) as determined in the XPS spectra of species B [7]. The singlet and triplet states of $[(HO)_4OSi_2O_2–Mo]^{2+}$ have been explored. The ground state is the triplet, separated by 0.68 eV from the excited singlet (Table 2 and Fig. 11). The bond of Mo to O_{3c} is even stronger than in the previous case as shown by the very short Mo–O distance of 2.16 Å (Fig. 11(a)). This is not surprising given the +2 actual charge on Mo and the formal +IV OS. The interaction energy with CO is comparable to that found for neutral or singly charged species, about 1.5 eV. The Mo–CO distance, however, becomes 2.16 Å (it was 2.09 Å on the singly charged complex and 1.98 Å on the neutral form). This means that two different bonding mechanisms occur, with a stable binding energy as a net result. On the neutral form, the back donation dominates and the Mo–CO distance is short, a very small electrostatic contribution is expected in this case. On the doubly charged complex, the electrostatic mechanism dominates and the back donation is practically absent due to the long Mo–CO distance and to the negligible d_π-CO $2\pi^*$ overlap. The singly charged complex is in between, with both mechanism acting

Table 2
Electronic properties of CO adsorbed on cluster models of Mo atoms bound on the surface of a SiO_2 support[a]

Species	Model	E_r (eV)	N_s	D_e (eV)	$\Delta\nu$ (cm^{-1})
Mo(II)	$[(HO)_4OSi_2O_2–Mo]–CO$	0.83	0	1.83	−222
Mo(II)	$[(HO)_4OSi_2O_2–Mo]–CO$	0.00	2	1.90	−215
Mo(II)	$[(HO)_4OSi_2O_2–Mo]–2CO$	0.83	0	3.69[b]	−224, −155
Mo(III)	$[(HO)_4OSi_2O_2–Mo]^+–CO$	0.00	1	1.73	−41
Mo(IV)	$[(HO)_4OSi_2O_2–Mo]^{2+}–CO$	0.68	0	1.82	+58
Mo(IV)	$[(HO)_4OSi_2O_2–Mo]^{2+}–CO$	0.00	2	1.52	+116

[a] E_r: relative energy with respect to the ground state; N_s: number of unpaired electrons; D_e: CO adsorption energy; $\Delta\nu$: harmonic CO vibrational frequency shift with respect to the free molecule. Calculated values for the gas phase CO molecule: $r_e = 1.127$ Å, $\nu = 2221\,cm^{-1}$.

[b] Energy required to dissociate both CO molecules.

at the same time. Given this analysis, it is not surprising that in $[(HO)_4OSi_2O_2–Mo]^{2+}$, the CO vibrational frequency is blue-shifted by +58 and +79 cm^{-1}, respectively, for the singlet and triplet states. This implies that charged Mo(IV) species may be responsible for band observed at 2170 cm^{-1}. In a similar way, the theoretical results do not support the assignments done in [10,36] where the bands shifted by +34, +38 and +60 cm^{-1} are tentatively attributed to Mo(III), Mo(IV) and Mo(V) species, unless they really are in a cationic form.

4. Conclusions

The vibrational frequencies of CO adsorbed on different models of Mo-based catalysts have been studied by DFT cluster model calculations. Only negative frequency shifts with respect to free CO have been found for CO bound to neutral Mo-containing species. The only exception is that of the MoO_3 molecule where a positive shift has been found in correspondence of a Mo atom in +VI formal oxidation state. This result can be rationalized with a pronounced ability of the Mo atom to back donate charge to the antibonding levels of CO even when the Mo atom is in a relatively high formal oxidation state. A blue-shift of the CO stretching frequency is found when charged species are present on the silica support. In this case, the electric field arising from the charge on the metal cation interacts electrostatically with the CO dipole moment leading to a substantial increase in the vibrational frequency. Candidates for the band observed at low-energy, 1990 cm^{-1}, are, therefore, CO molecules adsorbed on two-coordinated neutral Mo(II) atoms. It must be noted also that the intensity of the low-energy band increases when the reduction time increases [11]. Likewise, the $Mo(CO)_6$ species cannot be ruled out as the one that is responsible of the band at 1990 cm^{-1}. The CO stretching frequencies calculated for this complex are 2070 and 2183 cm^{-1}, rather close to the experimental values for the same complex in the gas phase (2000, 2025 and 2121 cm^{-1}) and also to some of the peaks — 1990, 2030, 2120 cm^{-1} — corresponding to the Mo supported species.

In summary, the assignment of the CO stretching bands corresponding to CO molecules interacting with supported Mo atoms is far from being a simple task. However, computational models such as those used in the present work provide important useful information that may help to interpret the experimental measurements and to gain further understanding about the role of the support in supported metal catalysts.

Acknowledgements

This research has been supported by the Spanish DGICYT grant PB98-1216-C02-01 and, in part, by Generalitat de Catalunya grant 1999SGR-00040 and "Integrated Action Spain–Italy" (HI1998-0042)". Part of the computer time was provided by the Centre de Supercomputació de Catalunya, CESCA, and Centre Europeu de Paral.lelisme de Barcelona, CEPBA.

References

[1] V.E. Henrich, P.A. Cox, The surface Science of Metal Oxides, Cambridge University Press, Cambridge, 1994.
[2] R.M. Lambert, G. Pacchioni, Chemisorption and Reactivity of supported clusters and thin films NATO ASI Series E, Vol. 331, Kluwer, Dordrecht, 1997.
[3] J. Haber, in: H.F. Barry, P.C.H. Mitchell (Eds.), Proceedings of the Climax 3rd International Conference on the Chemistry and Uses of Molybdenum, Climax Molybdenum Company, Ann Arbor, 1979, p. 114.
[4] M. Yamada, J. Yasumaru, M. Houalla, D.M. Hercules, J. Phys. Chem. 95 (1991) 7037.
[5] Yu.Y. Yermakov, Catal. Rev. Sci. Eng. 13 (1976) 77.
[6] Y. Iwasawa, Advan. Catal. 35 (1987) 187.
[7] J.M. Aigler, J.L. Brito, P.A. Leach, M. Houalla, A. Proctor, N.J. Cooper, W.K. Hall, D.M. Hercules, J. Phys. Chem. 97 (1993) 5699.
[8] J.L. Brito, B. Griffe, Catal. Lett. 50 (1998) 169.
[9] M.C. Kung, H. Kung, Catal. Rev. Sci. Eng. 27 (1985) 425.
[10] M.I. Zaki, B. Vielhaber, H. Knözinger, J. Phys. Chem. 90 (1986) 3176.
[11] C. Louis, L. Marchese, S. Coluccia, A. Zecchina, J. Chem. Soc. Faraday Trans. I 85 (1989) 1655.
[12] G. Ghiotti, E. Garrone, C. Morterra, A. Zecchina, J. Phys. Chem. 83 (1979) 2363.
[13] N. Echoufi, P. Gehin, J. Chem. Soc. Faraday Trans. 88 (1992) 1067.
[14] T.P. Beebe, P. Gehin, J.F. Yates, Surf. Sci. 148 (1984) 526.
[15] A.A. Tsyganenko, Russian J. Phys. Chem. 56 (1982) 1428.
[16] I.N. Senchenya, B. Civalleri, P. Ugliengo, E. Garrone, Surf. Sci. 412/413 (1998) 141.
[17] N. Lopez, G. Pacchioni, F. Maseras, F. Illas, Chem. Phys. Lett. 294 (1988) 611.
[18] N. Lopez, F. Illas, G. Pacchioni, J. Am. Chem. Soc. 121 (1999) 813.
[19] N. Lopez, F. Illas, G. Pacchioni, J. Phys. Chem. B 103 (1999) 1712.

[20] G. Pacchioni, N. Lopez, F. Illas, J. Chem. Soc. Faraday Discuss. 144 (1999) 209.
[21] N. Lopez, F. Illas, G. Pacchioni, J. Phys. Chem. B 103 (1999) 8552.
[22] A.D. Becke, Phys. Rev. A 38 (1988) 3098.
[23] C. Lee, W. Yang, R.G. Parr, Phys. Rev. B 37 (1988) 785.
[24] N. Lopez, F. Illas, J. Phys. Chem. B 102 (1998) 1430.
[25] N. Lopez, F. Illas, N. Rösch, G. Pacchioni, J. Chem. Phys. 110 (1999) 4873.
[26] P.L. Gunter, J.W. Niemantsverdriet, F.H. Ribeiro, G.A. Somorjai, Catal. Rev. Sci. Eng. 39 (1977) 77.
[27] J.Y. Carriat, M. Che, M. Kermarec, M. Verdaguer, A. Michalowicz, J. Am. Chem. Soc. 120 (1998) 2059.
[28] J. Sauer, P. Ugliengo, E. Garrone, V.R. Saunders, Chem. Rev. 94 (1994) 2095.
[29] W.J. Hehre, R. Ditchfield, J.A. Pople, J. Chem. Phys. 56 (1972) 2257.
[30] J.S. Binkley, J.A. Pople, W.J. Hehre, J. Am. Chem. Soc. 102 (1980) 939.
[31] P.J. Hay, W.R. Wadt, J. Chem. Phys. 82 (1985) 284.
[32] D. McLean, G.S. Chandler, J. Chem. Phys. 72 (1980) 5639.
[33] M.J. Frisch et al., Gaussian 94, Gaussian Inc., Pittsburgh, PA, 1997.
[34] G. Pacchioni, G. Cogliandro, P.S. Bagus, Int. J. Quant. Chem. 42 (1992) 1115.
[35] G. Herzberg, Spectra of diatomic molecules, Van Nostrand Reinhold, New York, 1950.
[36] E. Guglielminotti, E. Giamello, J. Chem. Soc. Faraday Trans. 181 (1985) 2307.